JOURNAL OF APPLIED ELECTROCHEMISTRY 13 (1983) 325–335

Aspects of the deposition of nickel on iron powder in a fluidized bed

L. CIFUENTES, A. J. FLETCHER

Department of Metallurgy, Sheffield City Polytechnic, Pond Street, Sheffield, UK

Received 23 November 1981; revised 13 September 1982

An examination has been made of the effect of the composition, pH and the temperature of the solution on the deposition of nickel on iron in a fluidized bed that contained iron powder, solution and a fluidizing gas. In certain cases an electric potential was applied to electrodes contained within the bed, but otherwise the deposition process was spontaneous*. Three different solutions were studied: nickel chloride, Watt's solution and nickel sulphamate. In the electroless case the highest and lowest deposition rates obtained under a specific set of experimental conditions were associated with the nickel chloride and nickel sulphamate solutions respectively. Even when an electric current was passed through the bed the spontaneous reactions dominated the process. The optimum pH was about 3.6; at other pH values the deposition of nickel was affected adversely by competitive cathodic reactions. The activation energies suggested that the deposition of nickel on iron powder was charge transfer controlled at temperatures below 60° C, but mixed diffusion and charge transfer control were operative at higher temperatures. The morphology of the coating was independent of the experimental conditions used, and always consisted of a nodular deposit giving incomplete coverage of the particles.

Nomenclature

A area of deposition surface (m^2)
c nickel concentration in solution (kg m^{-3})
c_0 initial nickel concentration in solution (kg m^{-3})
E° standard electrode potential (V)
k rate constant (m s^{-1})
m slope of Arrhenius plot (K)
Q activation energy (J mol^{-1})
r radius of powder particles (m)
R gas constant (J mol^{-1} K^{-1})
T temperature (K)
V solution volume (m^3)
A_1 total surface area of powder (m^2)
A_2 corrected total surface area of powder (m^2)
h pit depth (m)
M_t total mass of coated powder (kg)
N number of particles
N_p number of pits per particle
r_0 initial radius of particle (m)
r_1 final (uncorrected) radius of particle (m)
r_2 final corrected radius of particle (m)
r_p radius of pits (m)
V_{Ni} volume of deposited nickel (m^3)
V_1 volume of deposited layer (m^3)
Ni quantity of nickel in coated powder (mass%)
ρ_{Ni} density of solid nickel (kg m^{-3})

* Spontaneous is here taken to mean processes that do not require the use of feeder electrodes.

1. Introduction

The aim of the work reported here has been the study of the effect of certain process variables on the deposition of nickel on iron powder in a three-phase fluidized bed, the construction and characteristics of which have been the subject of a previous publication [1]. This earlier work clearly showed that when an electric potential was applied to the cell a significant proportion of the nickel deposited on the iron powder was obtained by a spontaneous cementation reaction, namely $Fe + Ni^{2+} \rightarrow Ni + Fe^{2+}$. The present work includes a more detailed study of the interaction of the cementation reaction and those due to the applied current as well as an examination of the effect of the major processing

0021–891X/83 $03.00 + .12. © 1983 Chapman and Hall Ltd.

variables on the deposition reactions. This allows the identification of the optimum conditions under which deposition of nickel should take place. The composition variations studied have been directed towards the examination of alternative solutions, not normally used in commercial nickel plating operations, which may allow the use of cheap feedstocks prepared from recycled material.

In chloride solutions the possible reactions include:

Cathodic	E° at 298 K and unit activities (V)	
$Ni^{2+} + 2e^- \rightarrow Ni$	−0.25	(a)
$2H^+ + 2e^- \rightarrow H_2$	0.00	(b)
$\frac{1}{2}O_2 + 2H^+ + 2e^- \rightarrow H_2O$	1.23	(c)
$\frac{1}{2}O_2 + H_2O + 2e^- \rightarrow 2OH^-$	0.40	(d)
Anodic		
$Ni \rightarrow Ni^{2+} + 2e^-$	−0.25	(e)
$H_2O \rightarrow \frac{1}{2}O_2 + 2H^+ + 2e^-$	1.23	(f)
$2Cl^- \rightarrow Cl_2 + 2e^-$	1.36	(g)
$Fe \rightarrow Fe^{2+} + 2e^-$	−0.44	(h)

When feeder electrodes are used the favoured anodic reaction is Reaction e, which leads to the dissolution of the nickel anode. Reaction h is normally prevented by the use of a membrane which separates the iron powder from the anode, although a small quantity of powder does penetrate this membrane.

At the cathode the favoured Reaction a involves the deposition of nickel but the ease with which the competing reactions occur is influenced by the pH of the solution. Thus Reaction c is favoured when the pH is high while Reaction b requires a low pH [2]. Both Reaction c and d require the presence of dissolved oxygen in the electrolyte.

When the movement of the iron particles in the fluidized bed brings each periodically into either direct or indirect contact with the cathode rods they become subject to the cathode reactions; in particular Reaction a, which leads to nickel deposition during the time that the particle is in contact with the current feeder. However, when the iron particles are suspended in the solution away from the cathode then Reaction h combines with Reaction a to give a simultaneous corrosion deposition process with both anodic and cathodic sites on the same particle. The spontaneous dissolution of iron at the anodic sites provides the driving force for the nickel deposition at the cathodic sites. Reactions b, c and d, previously referred to in connection with Reaction a may also compete with reactions at the cathodic sites on the powder, provided conditions are suitable.

In the absence of the current feeder electrodes the reactions are, of course, confined to those related to iron particles out of contact with the electrodes, namely iron dissolution at the anode sites and various combinations of the cathodic reactions at the cathodic sites. Again, deposition of nickel by Reaction a is the predominant cathodic reaction.

The production of an excess of OH^- ions by means of Reactions b, c and d may cause a local increase in the pH in the vicinity of the iron particles and may lead to the deposition of iron or nickel hydroxide on the surface of the particle by means of either of the reactions:

$$Fe^{2+} + 2OH^- \rightarrow Fe(OH)_2$$

$$\text{or } Ni^{2+} + 2OH^- \rightarrow Ni(OH)_2$$

The excessive production of such constituents on the surface would hinder nickel deposition on the surface of the powder. However, the presence of Cl^- ions counteracts this passivation process [3].

2. Experimental procedure

2.1. *Cell used to deposit nickel on iron powder*

Both spontaneous and electrolytic deposition was carried out in the same basic cell, the design of which is shown in Fig. 1.

The base of the chamber consisted of a porous disc through which an inert gas entered the cell under pressure. The passage of gas through the cell produced violent agitation of the electrolyte and the iron powder contained therein, which led to the establishment of a virtually uniform distribution of the latter through the bed. The random movement of the powder particles brought them periodically into contact with the 18/8 niobium

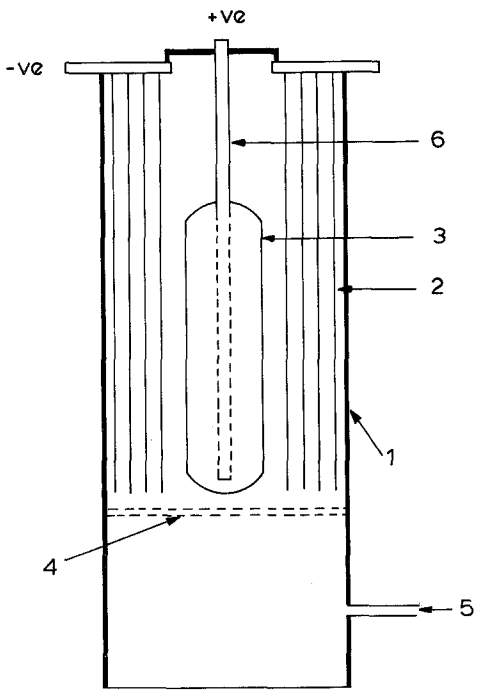

Fig. 1. Three-phase fluidized bed. 1, perspex tube; 2, cathode rods; 3, anode bag; 4, fluidizing membrane; 5, gas inlet tube; 6, anode rod.

stainless steel cathode rods, of which there were 24 with a diameter of 0.32 cm and length of 30 cm. The central anode, which consisted of nickel shot, was separated from the cathode region by a fabric membrane, which prevented contact between the iron powder and the nickel anode. The whole chamber was contained within a water bath, which was also used to heat the incoming gas.

The mass of powder and the volume of solution used in each experiment was 0.30 kg and 2.0 dm^3 respectively, but the expanded volume of the latter when the bed was fluidized was 3.0 dm^3, the maximum height of this expanded bed was approximately 15 cm. The specific surface area of the powder, the calculation of which assumed that the particles were spherical, was 13.3 $m^2\ kg^{-1}$. In cases where an applied current was used this was maintained at 10 A, while the gas flow rate was maintained in all cases at $1.3 \times 10^{-4}\ m^3\ s^{-1}$. A full description of the construction and characteristics of the cell has been previously published elsewhere [1].

2.2. *Deposition in the absence of an applied potential*

The same basic cell was also used to deposit nickel on iron powder by a spontaneous process, except that both anode and cathode assemblies were removed from the chamber.

2.3. *Solutions*

Three types of solution, the compositions of which are shown in Table 1, were used to produce both electrolytic and spontaneous deposition. Two were standard mixtures used in nickel electroplating baths while the third contained only nickel chloride. In certain cases additions of hydrochloric acid or sodium hydroxide were made to the above solutions in order to adjust the hydrogen ion concentration.

2.4. *Iron powder*

Atomet iron powder, supplied by Metal Powders Ltd, was used throughout: the composition and sieve analysis are given in Table 2.

2.5. *Chemical analysis of coated powder*

Samples of powder were removed periodically from the cell, washed with distilled water and finally with alcohol, followed by drying in air at 150° C. The nickel content of samples of both this powder and the solutions were determined by means of spectrophotometry of the oxidized nickel dimethylglyoxime complex. The iron content of the solutions was also determined using flame atomic absorption. The methods used did not differentiate between deposited metal and precipitated hydroxide.

2.6. *Metallographic examination of the powder surfaces*

Each powder sample was sprinkled on the plane surface of a metallic mounting covered by a thin layer of colloidal silver and then observed with a scanning electron microscope (SEM). The colloidal silver acted as a glue, which attached the powder to the mounting and at the same time provided the electrical conductivity required by

Table 1. Compositions of the solutions used

Watts solution		*'Sulphamate' solution*		*Nickel chloride solution*	
Compound	*concentration* ($g\ dm^{-3}$)	*compound*	*concentration* ($g\ dm^{-3}$)	*compound*	*concentration* ($g\ dm^{-3}$)
$NiSO_4 7H_2O$	150	$Ni(NH_2SO_3)_2 4H_2O$	195	$NiCl_2 6H_2O$	150
H_3BO_3	30	H_3BO_3	30		
NH_4Cl	30				

the SEM probe. The EDAX attachment was used to determine the composition at selected points on the powder particle surface.

3. Results

Figures 2a, b and c and 3a, b and c show the effect of time and temperature on the quantity of nickel deposited* on iron powder in each of the three solutions under consideration. In the case of Fig. 2 an electric potential of about 3 V was applied between cathode and anode, while the results shown in Fig. 3 were obtained spontaneously. Each result shown in Figs. 2 and 3 was the mean of two values, the degree of scatter being always less than ± 5%. A similar degree of scatter was obtained in the case of the results shown in Figs. 4, 5 and 6, which were also the means of duplicated values.

The overall rate of deposition on the iron powder in the presence of an applied current at a particular temperature varied markedly with the type of solution used, the highest and lowest deposition rates were obtained from the nickel chloride and 'sulphamate' baths respectively. The difference between these two extremes was substantial, being an order of magnitude at 62° C. The rates of deposition in both the Watts' and the 'sulphamate' baths showed a steady reduction as the plating time increased, and in all cases the rate of deposition increased as the temperature of the electrolyte increased. However, this latter effect was most marked in the case of the nickel chloride solution (Fig. 2c), particularly at temperatures above about 54° C.

The quantities of material referred to in Fig. 2 include only the nickel deposited on the iron powder, so that material deposited on the cathode rods has been excluded. The maximum possible quantities of deposited material resulting from the

Table 2. Composition and sieve analysis of iron powder

Composition		*Sieve analysis*	
Element	*Percentage present (mass%)*	*Mesh size* (μm)	*Percentage present (mass%)*
Fe	Balance	+ 150	8.31
Si	0.01	150–125	7.46
P	0.05	125–90	27.45
Mn	0.08	90–75	14.41
Ni	0.09	75–53	19.51
C	0.063	53–45	3.40
S	0.006	– 45	19.45
O	0.2		

* The mass of nickel deposited is expressed throughout as a percentage of the total mass of powder in the bed.

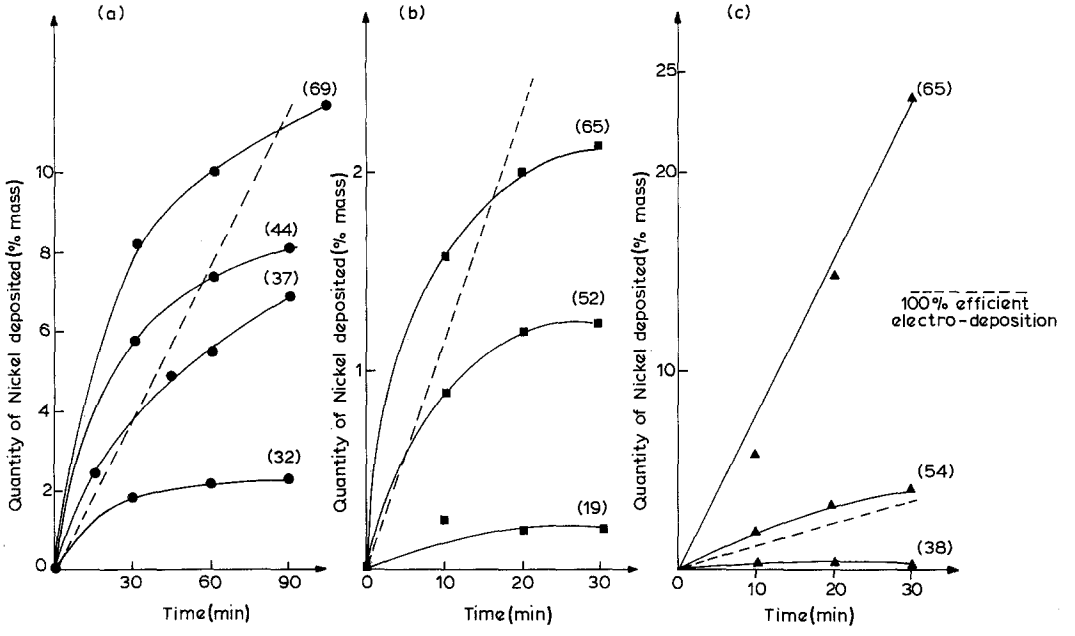

Fig. 2. The effect of time and temperature on the electrolytic deposition of nickel on iron powder in: (a) Watt's solution, (b) 'sulphamate' solution, (c) nickel chloride solution, (Figures in brackets refer to temperature in ° C).

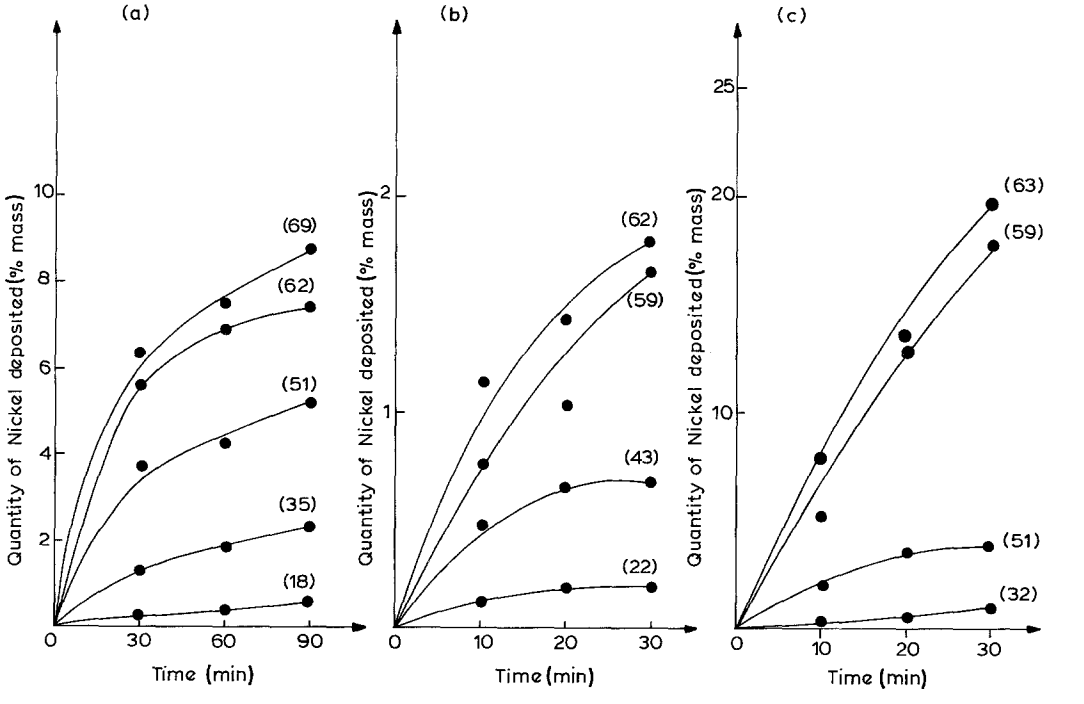

Fig. 3. The effect of time and temperature on the spontaneous deposition of nickel on iron powder in: (a) Watt's solution, (b) 'sulphamate' solution, (c) nickel chloride solution, (Figures in brackets refer to temperature in ° C).

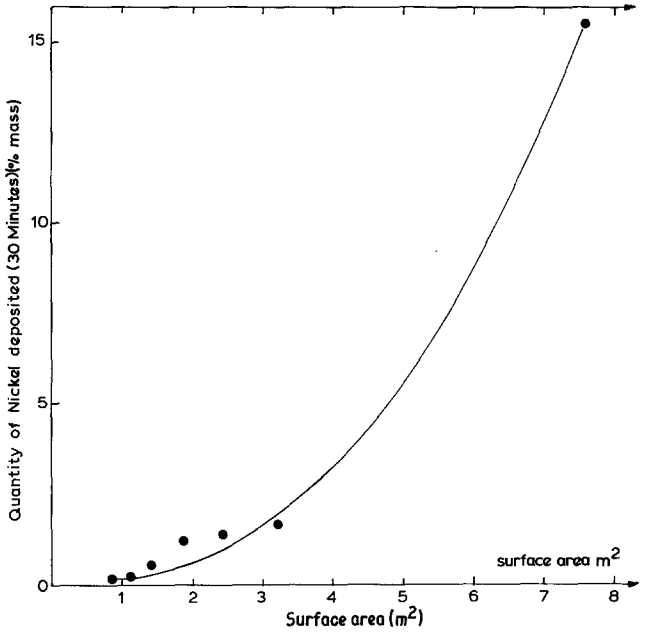

Fig. 4. The effect of surface area on nickel deposition under spontaneous conditions.

passage of the applied current (shown by dotted lines in Figs. 2a, b and c) included deposits at all sites in the cell, so that these quantities represent over-estimates of the amounts of nickel that could be deposited on the powder as a result of the passage of the current.

The relationships between time, temperature and quantity of nickel deposited from all three solutions in the absence of an electric current (Fig. 3) were very similar to those obtained when a current passed between the electrodes (Fig. 2). Thus, again, nickel chloride gave the highest rate under a specific set of experimental conditions and the 'sulphamate' solution gave the lowest. A reduction in the rate of deposition was again observed as the time increased, although this effect was now also obtained to a limited extent with the nickel chloride solution. The effect of temperature on the rate of deposition followed closely the results obtained when a current was passed between the cell electrodes.

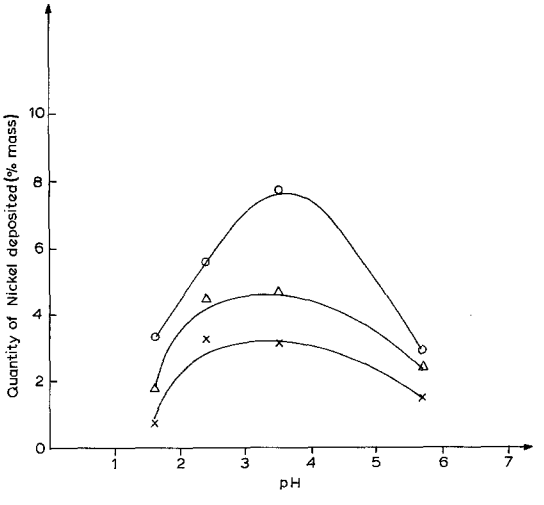

Fig. 5. The effect of pH on the quantity of spontaneous deposition from nickel chloride solutions after times of up to 30 min at 62° C. ×, 10 min; △, 20 min; ○, 30 min. Solution; Nickel chloride, 150 g dm^{-3}. Powder particle size ⩽ 45 μm.

Figure 4 shows the effect of the total surface area of the particles on the deposition of nickel in the absence of an externally applied current. A linear relationship between the quantity of deposited nickel and the total surface area was expected since [4–7]:

$$\text{deposition rate} = \frac{KAc}{V}$$

The relationship between the mean deposition rate during the first 30 min of the process and the surface area of the particles was not linear, although this departure from linearity was mainly due to the enhanced rate of deposition obtained when the finest particles were used.

In the absence of any applied current the rate of deposition of nickel was sensitive to the

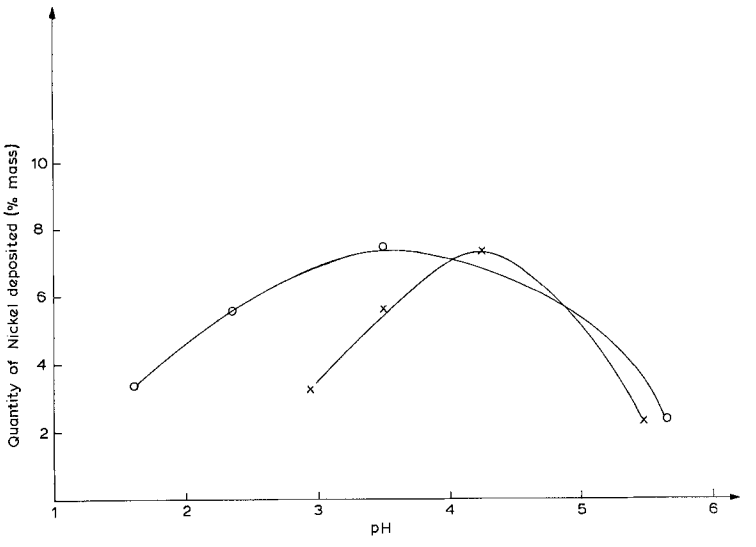

Fig. 6. The influence of hydrogen evolution on the pH of the nickel chloride
o, initial pH of solution;
X, average pH values during complete deposition process.

hydrogen ion concentration of the solution. Fig. 5 shows that the quantity of nickel deposited from nickel chloride solutions after a fixed time of 30 min at 62° C reached a maximum when the initial pH of the solution was 3.6, although the results obtained at shorter times suggest that the maximum rate of nickel deposition occurred within the pH range of 2.4–3.6.

When solutions with low initial values of pH were used the early stages of the process involved intense hydrogen evolution, although this reaction slowed down and eventually ceased. This period of hydrogen evolution was associated with a significant increase in pH so that the average value was significantly higher than that obtained initially (Fig. 6).

The relationships between the concentrations of nickel ions in the solution and the reaction times in the case of spontaneous deposition from both the nickel chloride and Watts' solutions indicate that a first-order reaction was involved.

Thus Fig. 7 shows almost invariably a linear relationship between $\text{Log}\, c/c_0$ and time. The reduction in nickel ion concentration produced by the deposition process was partially counteracted by the evaporation of the solutions.

Table 3 indicates that the amount of nickel deposited in 30 min may be significantly increased by an increase in the initial nickel chloride concentration from 150 g dm^{-3} to 250 g dm^{-3}, the magnitude of this effect was considerably greater than that suggested by a first order reaction.

The morphology of the deposit on the surface of the iron powder was not significantly influenced by variations in temperature, solution composition, or particle size, within the ranges of these parameters studied during the present investigation. In all cases a nodular deposit was produced, a typical example of which is shown in Fig. 8.

As the amount of nickel deposited increased the protuberances grew in size, but did not develop the dendritic shape obtained with some other deposits [4]. The extremely irregular shape of the iron powder particles made it difficult to compare accurately the relative proportions of nickel and iron on different parts of the specimen, but there was evidence that the nodular protrusions were very rich in nickel, while the recesses were not (Table 4).

Since the probe detected both the nickel coating and an unspecified quantity of the iron beneath, these readings provided only qualitative evidence of the variation in nickel content on the surface of the powder. The differences detected were, however, substantial and do indicate a clear lack of uniformity in the coating at different points on the surface.

4. Discussion

The rate of spontaneous deposition fell slightly as the plating time increased (Fig. 3). This effect

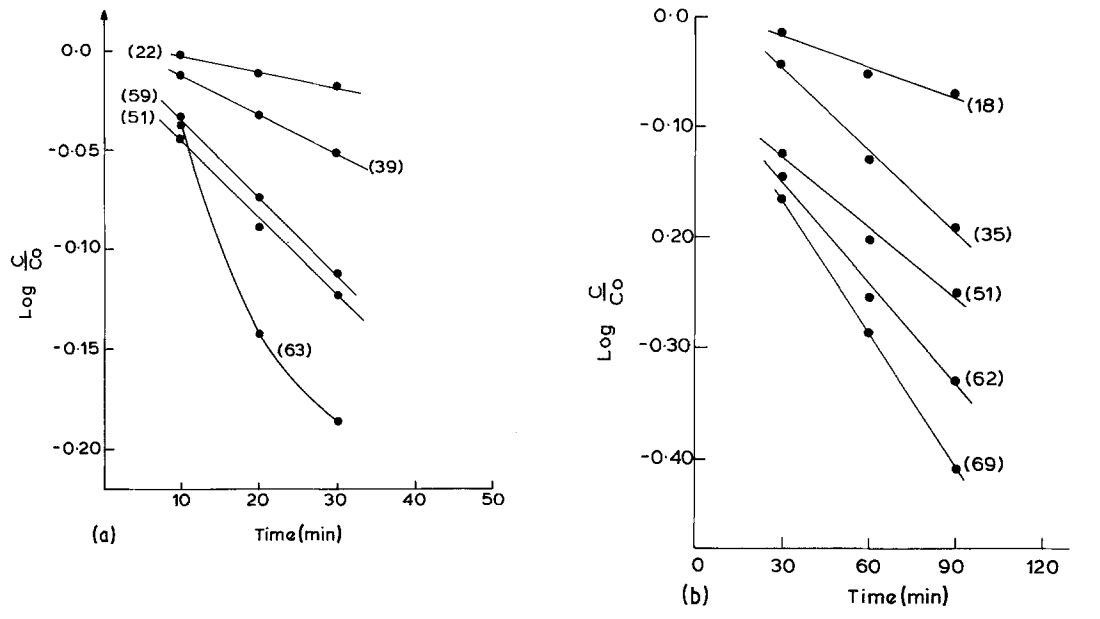

Fig. 7. The relationships between Log C/C_0 and time in: (a) nickel chloride solution, (b) Watt's solution, (figures in brackets refer to temperature in ° C).

may be explained by a reduction in the Ni^{2+} concentration in the solution and the formation of a layer of deposit on the surface of the powder.

Since the magnitude of the reduction in the deposition process was smallest when the reduction in the nickel concentration was greatest (i.e., in nickel chloride) it would appear that the influence of the deposit on the rate of further deposition was significant in the later stages of the process, even though no evidence has been obtained of a complete layer of nickel on the surface of the iron powder. Fig. 8, which shows an irregular nodular deposit, was typical of the morphology of the powder surface after deposition had taken place. Despite the complexity of the deposition process on the surface of the powder, the reaction kinetics, followed by the measurement of the concentration of cations in the solution, suggested a first-order reaction (Fig. 7).

The effect of time on the rate of deposition of nickel in the presence of an electric potential was very similar to the results obtained using spontaneous deposition only, which was probably due to the dominance of the latter, even when a potential was applied to the electrodes. A comparison of Figs. 2 and 3 suggests that the spontaneous contribution to the deposition process was as much as 80% of the total. The mechanism by which charge is passed in a fluidized bed is complex [8] but the spontaneous dissolution of iron is not prevented by the passage of current, except when the powder particles make contact with the cathode or with negatively charged particles, which would provide cathodic protec-

Table 3. Effect of nickel chloride concentration on the quantity of nickel deposition at 52° C (30 min)

Concentration of nickel chloride (g dm^{-3})	*Quantity of 'Electrolytic' deposition** (mass% Ni)	*Quantity of spontaneous deposition* (mass% Ni)
150	7.5	3.7
250	22.8	16.7

* This includes a substantial spontaneous component.

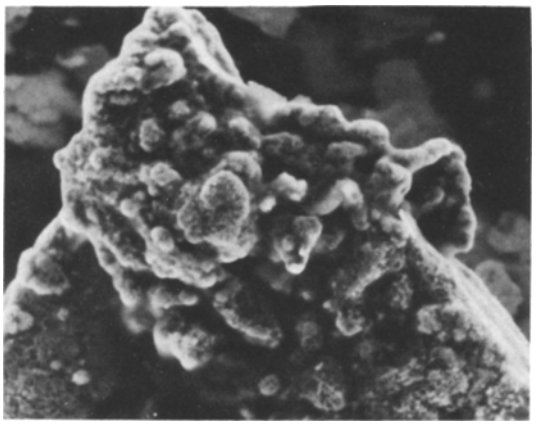

Fig. 8. Morphology of nickel deposited from a solution of optimum pH (magnification × 1888).

tion. In the present case, with a relatively low density of particles in the bed, cathodic protection of the particles would persist for a relatively short proportion of the time.

The optimum nickel deposition rate occurred at intermediate pH levels in the solution, when interference from competing cathodic reactions was probably minimized. Lower pH values would encourage the reaction $2H^+ + 2e^- \rightarrow H_2$, while higher pH levels would lead to the formation of deposits of hydroxides on the powder surface. The Pourbaix diagram for iron [9] indicates that hydrogen ion discharge is favoured at $pH < 6$ while kinetic factors favour oxygen reduction at $pH > 7$ [2]. These results indicate that the optimum pH for nickel deposition should be considerably higher than the value obtained in the present investigation (about 3–3.5). The discrepancy is possibly due to the difference between the local and the bulk pH, the former being higher than the latter, due to the H^+ consuming cathodic reactions.

The relationships between the rates of nickel deposition and temperature have been used to determine the activation energies of the process by means of the Arrhenius relationship. Corrections were made for both the effect of change in solution volume by evaporation and the change in the surface area as the particles grew. The former effect was determined empirically from experimental data, while the latter was calculated by the method given in the appendix. The relationships between the logarithm of the rate constant k and $1/T$ are given in Fig. 9 and the activation energies are obtained from this data by the equation $-mR = Q$. It is evident from Fig. 9 that in no case was a single activation energy applicable over the whole temperature range, since abrupt changes in slope occurred at about 60° C. Similar phenomena have been reported by others investigating the cementation reaction on planar surfaces [4, 7, 10]. The magnitude of the activation energies shown in Table 5 suggest that the value at the lower temperature was always the higher, although both values were dependent upon the solution employed. The ranges of values obtained overall indicate that the 'low temperature' process was controlled by charge transfer, while the 'high temperature' process probably also possessed an element of diffusion control. Diffusion control is probably less likely in a highly agitated fluidized bed than in the case where spontaneous deposition takes place on planar surfaces, where the diffusion mechanism is well established [7, 10]. However, the presence of fine pores within the deposited layer, which provide the only contact between the iron and the solution would be an additional source of diffusion control [10].

The absence of a linear relationship between the quantity of deposited nickel and surface area

Table 4. Quantity of nickel detected by the SEM probe at points on the coated powder surface

Position on surface	$\frac{\text{Fe K peak height}}{\text{Ni K peak height}}$
Recess	∞
Recess	4.35
Protrusion	0.65
Protrusion	0.28
Protrusion	0.28

Table 5. Activation energies of the coating process

Solution	*'Higher' temperature range* (kJ mol^{-1})	*'Lower' temperature range* (kJ mol^{-1})
'Sulphamate'	9.6	56.3
Watt's	28.2	64.5
Nickel chloride	68.9	144.4

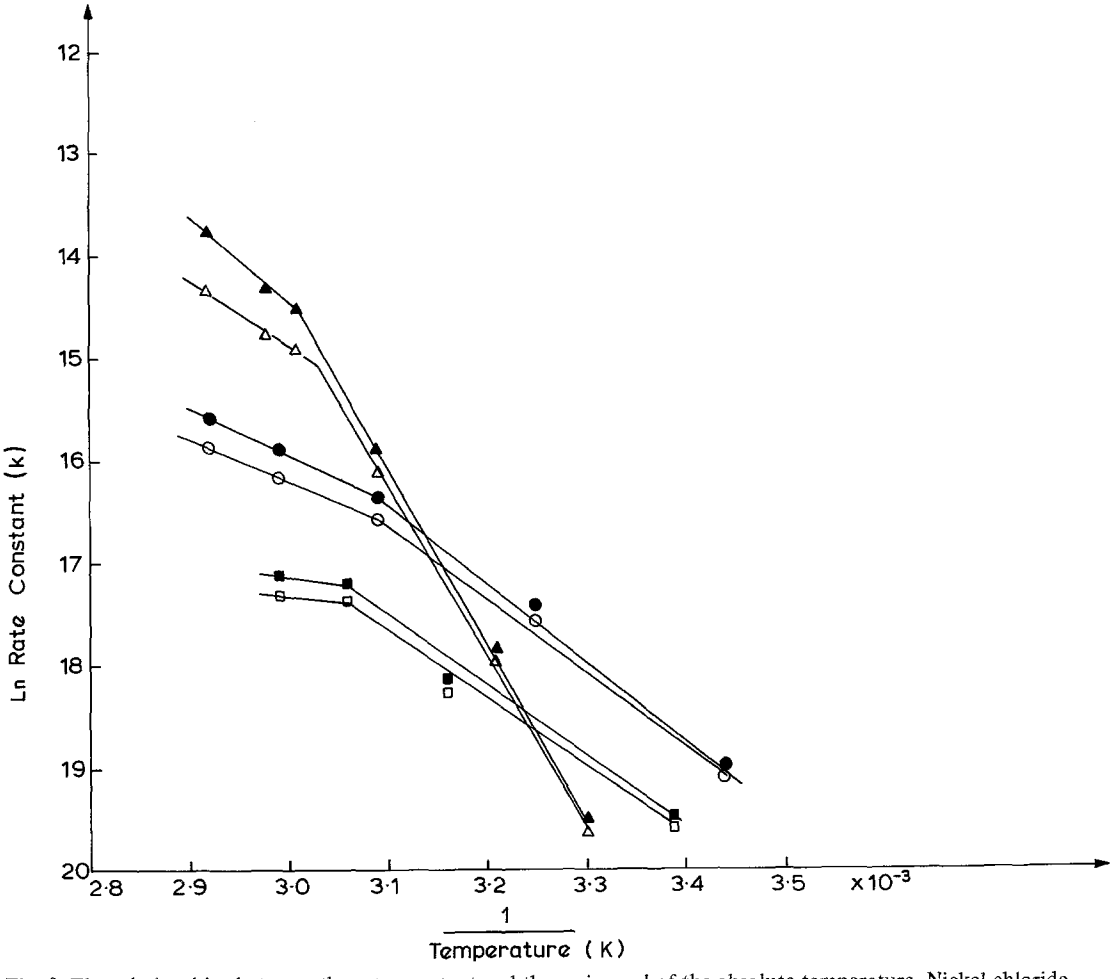

Fig. 9. The relationships between the rate constant and the reciprocal of the absolute temperature. Nickel chloride, ▲ apparent k, △ corrected k; Watt's solution, ● apparent k, ○ corrected k; sulphamate, ■ apparent k, □ corrected k.

(Fig. 4) suggests that the efficiency of the deposition process increases as the particles become smaller. Finer particles are more readily maintained in suspension and may produce a more efficient fluidized bed than coarse material. However, this aspect of the process is not yet clearly understood.

5. Conclusions

The most important conclusions of this study are:

(a) The overall rate of nickel deposition obtained is greatest in the case of the nickel chloride solution and least in the case of the sulphamate electroplating bath. These conclusions apply whether or not an electric potential is applied.

(b) The activation energies of the deposition processes suggest that charge transfer control operates at temperatures below 60° C while mixed diffusion and charge transfer control is present at higher temperatures.

(c) The rate of deposition of nickel from nickel chloride is at a maximum when the pH of the solution is about 3.6. At lower and higher pH levels competing cathodic reactions hinder the deposition of nickel.

(d) The relationship between the powder surface area and the quantity of deposited nickel is not linear, but shows enhanced nickel deposition as the surface area is increased.

Appendix

The surface area of the coated powder

If it is assumed that the powder particles are spherical and of uniform size then the total surface area is given by:

$$A_1 = 4\pi n r_1^2. \qquad \text{(A1)}$$

If it is also assumed that the deposited layer is continuous and uniform with a density equal to that of pure nickel then the volume of the deposited nickel is given by:

$$V_{Ni} = \frac{NiM_t}{100\,\rho_{Ni}} = \tfrac{4}{3}\pi N(r_1^3 - r_0^3). \qquad \text{(A2)}$$

However, the coating is irregular (Fig. 8). In an attempt to make a closer approximation to the actual morphology of the surface it has been assumed that the uncoated regions may be represented by cylindrical pits, all of the same size, that occupy half the surface of the particle. Since the volume actually occupied by deposit will then be half of a uniform layer of the same thickness

$$\tfrac{4}{3}\pi(r_2^2 - r_0^3) = \frac{NiM_t}{50\,\rho_{Ni}}. \qquad \text{(A3)}$$

Hence

$$r_2 = \left(\frac{3NiM_t}{200\,\rho_{Ni}}\pi N + r_0^3\right)^{1/3}$$

The area now covered by the deposited layer is equal to the sum of the area of the original particle and the area of the walls of the pits.

$$A_2 = 4\pi N r_2^2 + NN_p 2\pi r_p h. \qquad \text{(A4)}$$

As the pits occupy half the particle surface:

$$Np = \tfrac{1}{2}\left(\frac{4\pi r_2^2}{\pi r_p^2}\right) = \left(\frac{2r_2^2}{r_p^2}\right) \qquad \text{(A5)}$$

and

$$A_2 = 4\pi N r_2^2\left(1 + \frac{h}{r_p}\right).$$

Finally, if it is assumed that the depth of the pits is equal to the radius, the new surface area of the particle is given by $A_2 = 8\pi N r_2^2$

$$= 8\pi N\,\frac{(3NiM_t + r_0^3)^{2/3}}{200\,\rho_{Ni}\pi N}. \qquad \text{(A6)}$$

Acknowledgements

The authors wish to thank the Science and Engineering Research Council for the provision of a grant, without which this work would not have been possible. Grateful thanks are due also to Metal Powders Limited for the gift of the iron powder used in this investigation.

References

[1] A. J. Fletcher, S. Jaiswal and R. Cundill, in 'Modern Perspectives in Powder Metallurgy', Vol. 12, (edited by H. H. Hausner, H. W. Antes and G. D. Smith) Princeton American Powder Industries Federation, Princeton (1981) p. 177.

[2] J. O'M. Bockris and A. K. N. Reddy, 'Modern Electrochemistry, Vol. 2, Plenum, New York and London (1970) p. 1267.

[3] I. K. Vetter, 'Electrochimiques', Springer, Berlin (1961) p. 610.

[4] V. Annamalai, J. B. Hiskey and L. E. Murr, *Hydromet.* **3** (1978) 163.

[5] G. P. Power and I. M. Ritchie, in 'Modern Aspects of Electrochemistry', Vol. 11 (edited by J. O'M. Bockris and B. E. Conway) Plenum New York and London (1975).

[6] R. S. Rickard and M. C. Furstenau, *Trans. Met. Soc. AIME* **242** (1968) 1487.

[7] M. E. Wadsworth, *ibid.* **245** (1969) 1381.

[8] B. J. Sabacky and J. W. Evans, *Met. Trans. B*, **8B** (1977) 5.

[9] M. Pourbaix, 'Atlas de Equilibres Electrochim' Gauthier-Villars, Paris (1963).

[10] J. D. Miller, *Miner. Sci. Eng.* **5** (1973) 242.